crystals

MDPI

Article

The Crystallization Behavior of TiO_2-CaO-SiO_2-Al_2O_3-MgO Pentabasic Slag with a Basicity of 1.1–1.4

Huxu Lei [1], Chaowen Tan [1], Gangqiang Fan [1,2], Dejun Huang [3], Xiaoming Ding [4] and Jie Dang [1,2,*]

1 College of Materials Science and Engineering, Chongqing University, Chongqing 400044, China; 20183002@cqu.edu.cn (H.L.); 20183003@cqu.edu.cn (C.T.); fan_gangqiang@cqu.edu.cn (G.F.)
2 State Key Laboratory of Advanced Processing and Recycling of Non-Ferrous Metals, Lanzhou University of Technology, Lanzhou 730050, China
3 Spectris Instr. & Sys. Shanghai Ltd., Malvern Panalytical (China), Shanghai 200233, China; dejun.huang@panalytical.com
4 National Innovation (Qingdao) High Speed Train Material Research Institute Co., Ltd., Qingdao 266109, China; dingxiaoming@biam.ac.cn
* Correspondence: jiedang@cqu.edu.cn; Tel./Fax: +86-23-6511-2631

Abstract: The utilization of titanium-containing blast furnace slag has been an unsolved problem for a long time. Failure to make effective use of the slag, which is caused by a high TiO_2 content within it, not only results in a waste of resources, especially titanium, but also increases environmental risk. The key to address the problem is the enrichment and extraction of TiO_2 from the slag first. Therefore, in order to study the enrichment of titanium, the crystallization behavior of TiO_2-CaO-SiO_2-Al_2O_3-MgO pentabasic slag, the main compositions of titanium-containing blast furnace slag, within the basicity range of 1.1–1.4 was investigated theoretically and experimentally. Thermodynamic calculation shows that perovskite is the main titanium-containing phase and titanium can be enriched in perovskite. By decreasing the temperature, perovskite precipitates at first. Additionally, with the increase of basicity, perovskite precipitation temperature increases continuously, and its amount of precipitation almost does not change, while the amounts of other phases change obviously. The experimental results demonstrate similar results except for the amount of perovskite (with the increase of basicity, perovskite precipitation amount increases slightly), caused by kinetic reason. In addition, the morphology of the slag at different scales was observed. The surface of the cooled slag is granular, vein-like, and irregular, multilaterally shaped from outside to inside. The crystal is dendritic with a spine-like trunk, and the edge is blade-like. In terms of the structure of the crystal, the inner part of it is perovskite, and the outer part is covered with a layer of other phases with spinel inlaying it. Finally, the precipitated mechanism is proposed as well.

Keywords: blast furnace slag; basicity; crystallization; TiO_2

Citation: Lei, H.; Tan, C.; Fan, G.; Huang, D.; Ding, X.; Dang, J. The Crystallization Behavior of TiO_2-CaO-SiO_2-Al_2O_3-MgO Pentabasic Slag with a Basicity of 1.1–1.4. *Crystals* **2021**, *11*, 583. https://doi.org/10.3390/cryst11060583

Academic Editors: Heike Lorenz and Béatrice Biscans

Received: 19 April 2021
Accepted: 19 May 2021
Published: 22 May 2021

1. Introduction

The majority of titanium resource exists in the form of ilmenite, and China has the most vanadium titanomagnetite resource in the world, which can then be beneficiated to ilmenite and titanium-containing magnetite [1,2]. In the existing production process, titanium-containing magnetite is mainly used to smelt iron while producing large quantities of titanium-bearing blast furnace (BF) slag. Additionally, the BF slag is accumulated at a rate of around 5 million tons per year in China. Until now, the titanium-bearing blast furnace slag is accumulated up to 100 million tons, which contains more than 20 million tons of titanium dioxide, resulting in great waste of the titanium resource [3]. Basically, the common blast furnace slag is employed as a building material. However, for titanium-containing blast furnace slag, the high content of TiO_2 (more than 20 mass %) makes the slag not suitable for being a building material (a typical composition of Panzhihua Iron and Steel Group titanium-containing BF slag is listed in Table 1 [4]). To address these

issues, many methods have been put forward, including the traditional utilization methods such as acid leaching, alkali leaching, alloy preparation, and so on [5–8]. Additionally, the new methods of preparation of glass-ceramics, rutile, and porous ceramic photocatalysts have been proposed in recent years [9–14]. However, the application of those methods in industry still has many problems. Considering the prospect of industrialization, it is ideal to enrich titanium first and then to prepare titanium metal or its compounds by using electrochemical, carbonitriding, and other ways [15–18].

Table 1. The typical compositions of titanium-bearing blast furnace slag in Panzhihua Iron and Steel Group (wt.%).

CaO	SiO_2	MgO	Al_2O_3	TiO_2	Other	Total	R *
27.53	24.04	7.97	13.7	22.57	4.19	100	1.15

* $R = \frac{CaO(wt.\%)}{SiO_2(wt.\%)}$.

The binary basicity ($\frac{CaO(wt.\%)}{SiO_2(wt.\%)}$) of the initial blast furnace slag is around 1.1, and the main titanium-containing phases are perovskite, titanium-containing spinel, and a small amount of TiO_2. The complex distribution of titanium in slag and the fine and uneven titanium-containing phase particles affect the utilization of titanium. Basicity is a very essential factor, which can determine the initial precipitation temperature and the type of phase [19]. Therefore, the study of the effect of basicity on the enrichment of titanium in slag is very important for the subsequent separation of titanium-containing phases. However, to the best of our knowledge, the study on the influence of basicity on the distribution of titanium in the crystallization process is still insufficient. Therefore, in the current study, the influence of basicity varying from 1.1 to 1.4 on the crystallization behavior of TiO_2-CaO-SiO_2-Al_2O_3-MgO (the main composition of titanium-bearing BF slag) system was studied theoretically and experimentally, and the mechanism of its crystallization was proposed.

2. Materials and Methods

TiO_2-CaO-SiO_2-MgO-Al_2O_3 slags were prepared by using reagent-grade oxide powders of CaO (99.99 wt. pct Tianjing Bodi), SiO_2 (99.99 wt. pct Chengdu Kelong), MgO (99.99 wt. pct Chengdu Kelong), Al_2O_3 (99.99 wt. pct Chengdu Kelong), and TiO_2 (99.99 wt. pct Chengdu Kelong). The mass ratios of different basicity are shown in Table 2. Raw materials were calcined first for 24 h at 1273 K, and subsequently, around 40 g sample was weighed and placed into the molybdenum crucible with 45 mm in inner diameter and 50 mm in height. In the experiment, nitrogen was first injected into the furnace to discharge air, with the crucible being placed in the heating area of the furnace tube. When the heating officially began, the sample was melted in a segmenting manner by heating at 4 K/min to 1473 K (1200 °C) and then at 2 K/min to 1873 K (1600 °C). The mixture was then held in a nitrogen atmosphere for three hours to homogenize. Finally, the sample was cooled at a rate of 3 K/min [20]. The detailed schematic diagram of the experimental apparatus was present in our previous study [18].

Table 2. The compositions of the TiO_2-CaO-SiO_2-Al_2O_3-MgO slag (wt.%).

No.	TiO_2	CaO	SiO_2	MgO	Al_2O_3	R	R_4
1	24	28.29	25.71	8	14	1.1	0.91
2	24	29.45	24.55	8	14	1.2	0.97
3	24	30.52	23.48	8	14	1.3	1.03
4	24	31.5	22.5	8	14	1.4	1.08

$R = \frac{CaO(wt.\%)}{SiO_2(wt.\%)}$; $R_4 = \frac{CaO(wt.\%)+MgO(wt.\%)}{SiO_2(wt.\%)+Al_2O_3(wt.\%)}$; The basicity in following content represents R.

The compositions of the cooled samples were detected by X-ray diffraction (XRD) (PANalytical, AERIS, Almero, The Netherlands), with Cu Kα radiation. The morphologies and interior crystal distribution of these samples were observed using Scanning Electron

Microscopy (SEM; TESCAN VEGA 3 LMH, Thermo Fisher Scientific, Brno, Czech Republic and Quattro S). At least 15 images per basicity were obtained, and then the Python OpenCV module (Guido van Rossum, The Netherlands) was used to realize image contour recognition and area calculation. Finally, the crystal area ratio for different basicity was calculated.

3. Results and Discussion

3.1. Thermodynamic Calculation

To investigate the phase compositions of titanium-bearing BF slag in the temperature range from 1873 K (1600 °C) to 1273 K (1000 °C) in nitrogen atmosphere, the thermodynamic calculation was performed by using the equilibrium module in FactSage 8.0 (FToxid databases) (GTT-Technologies and Thermfact, Herzogenrath and Montreal, Germany and Canada), with the same compositions of TiO_2-CaO-SiO_2-MgO-Al_2O_3 used in experiments (Table 2). However, the FToxid database in Factsage 8.0 is not fully optimized for such a complex system as TiO_2-CaO-SiO_2-MgO-Al_2O_3; therefore, there are some errors in thermodynamic calculations. It can be found that during the cooling process, perovskite ($CaTiO_3$) is the first phase to precipitate from the liquid. As the crystallization process proceeds, titania-spinel phase, melilite phase, $CaAl_2Si_2O_8$, and clinopyroxene (olivine) phase precipitate accordingly, as shown in Figure 1a–d. Finally, at 1492 K (1219 °C), the crystallization process is finished, while the liquid phase disappears, and is transformed into perovskite, spinel, melilite (olivine), clinopyroxene, and $CaAl_2Si_2O_8$.

The initial crystallization temperature of the phases is shown in Figure 1e. For the titanium phases, as the basicity increases, the crystallization temperature of perovskite increases from 1707 K (1434 °C) to 1757 K (1484 °C), and the crystallization temperature of titania-spinel increases from 1598 K (1325 °C) to 1660 K (1387 °C). For other phases, the crystallization precipitation temperature does not change significantly.

The change of phase mass ratio with basicity is shown in Figure 1f. With the increase of basicity, the amount of $CaAl_2Si_2O_8$ phase decreases, while the amount of titania-spinel and melilite increases. When the basicity is 1.2, the amount of clinopyroxene precipitation reaches the peak, and then decreases continuously. However, with increasing basicity, the amount of perovskite barely changes.

Pseudo ternary phase diagram (in Figure 2) shows that the liquid phase is completely transformed to solid phase at 1492 K, and the precipitation amounts of perovskite phase, clinopyroxene phase, and spinel phase reach the maximum simultaneously. Taking the basicity of 1.3 as an example, the analysis of pseudo ternary phase diagram shows that the initial slag is at point A. With the decrease of temperature, the perovskite phase precipitates along line AB, and the rest of the liquid phase precipitates along line ACG initially with precipitating titanium-containing spinel and melilite. When reaching point G, ternary eutectic reaction occurs, and $CaTiO_3$, anorthite, and titanium-containing spinel begin to precipitate. Then, the liquid phase precipitates along the GDE line and the eutectic reaction occurs again at point E. When the temperature drops to the liquidus temperature (1492 K), crystallization is completed and the liquid phase disappears.

3.2. The Experimental Results

The X-ray Diffraction (XRD) results of different basicity were shown in Figure 3. The peaks of the five main phases were attached at the bottom of the figure. According to the analysis, the peak intensity ratio of perovskite and clinopyroxene increases with the increase of basicity.

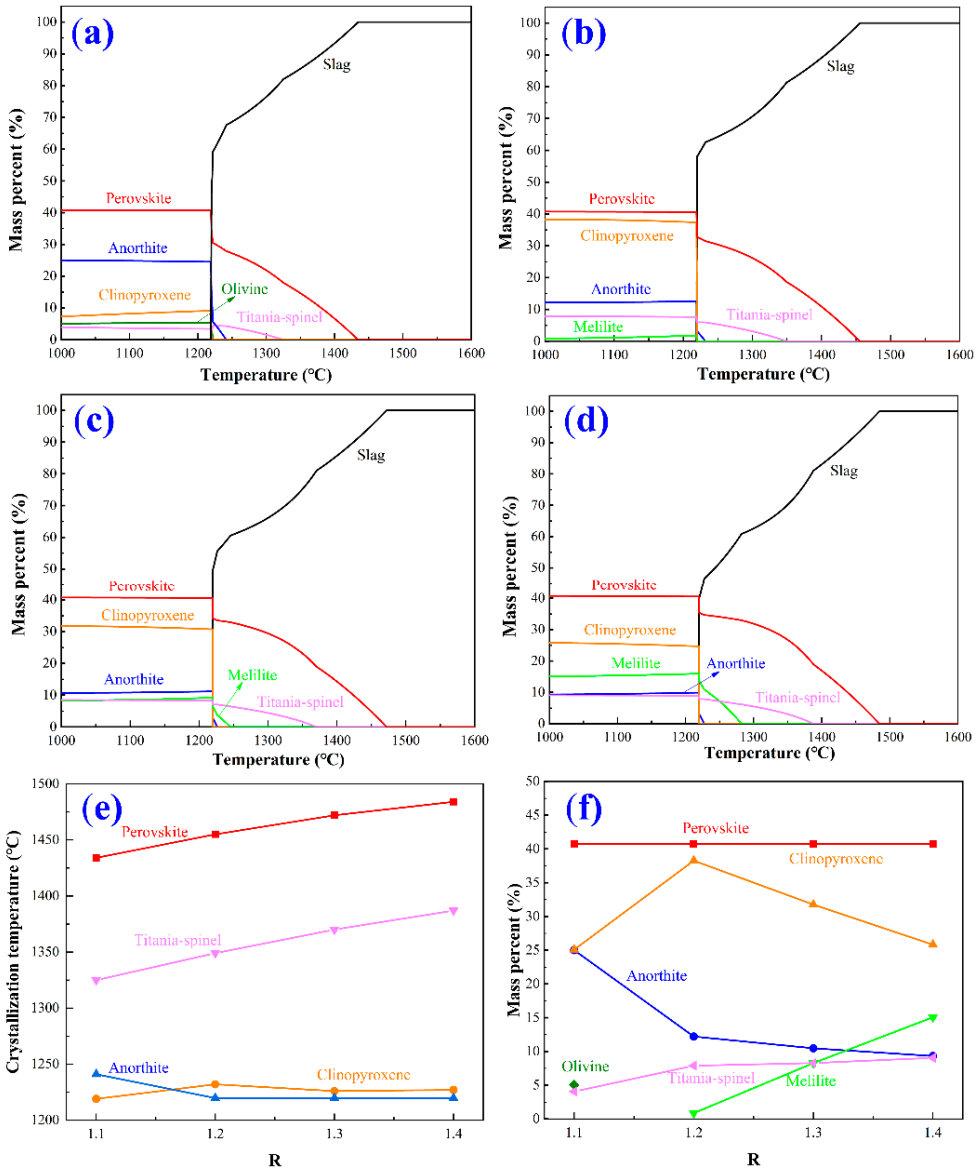

Figure 1. Thermodynamic calculation of TiO_2-CaO-SiO_2-Al_2O_3-MgO slag precipitation: theoretical phase compositions with basicity of (**a**) 1.1, (**b**) 1.2, (**c**) 1.3, (**d**) 1.4; (**e**) basicity dependence of crystallization temperature; (**f**) basicity dependence of mass percent of crystallized phases. (Perovskite-$CaTiO_3$, clinopyroxene-$Mg_2Si_2O_6$, $MgAl_2SiO_6$, $CaAlSi_2O_6$(+), $MgAlSi_2O_6$(+), $CaMgAlSiO_6$[−], Mg_2AlSiO_6[−], olivine-Mg_2SiO_4, anorthite-$CaAl_2Si_2O_8$, titania-spinel-$MgAl_2O_4$).

Macroscopic and microscopic observation was made on the crystal morphology of slags. The observation results of the crystal surface of slags are shown in Figure 3. It is found that along the radial direction of the crucible wall, the crystal morphology changes regularly. Taking basicity of 1.2 as an example, the outermost layer presents fine granular shape, and the inner layer presents vein shape, and the center presents irregular multilateral shape. The main reason is that the crucible wall has good thermal conductivity and heat dissipation ability during the cooling process, so that the outermost layer of the slag has a large supercooling degree. Considering the rough crucible wall, the outermost layer would form a large number of heterogeneous nucleation. After the formation of fine equiaxed grains on the surface, the temperature drops slowly and the transfer of heat to the outside becomes stable. The tiny nucleus grows along the central direction, thus forming the intermediate columnar grains. Finally, when the temperature drops below the liquidus, and as the solidification layer moves inward, the subcooling of components keeps

increasing. When the degree of subcooling was sufficient, the remaining liquid begins to crystallize, leading to the formation of internal equiaxed crystals.

Figure 4a presents the back-scattering image of the cross-section of cooled slag. It can be found that the white area exists in the form of a block and is surrounded by gray area. Besides, there are small parts of dark gray area. A number of feature points were selected for EDS (Dispersive Spectrometer Energy) analysis, as shown in Table 3. It can be obtained that the composition of the points A and B is $CaTiO_3$, C is $Ca_2MgSi_2O_7$, and D is $MgAl_2O_4$. A small amount of Ti element is also contained in C and D, which does not affect the main composition. Mapping results also confirm the above analysis (shown in Figure 4a–f). Additionally, thus, combined with EDS analysis, the white block area, the dark gray area, and the gray area correspond to $CaTiO_3$, $MgAl_2O_4$, and other phases ($CaMgSi_2O_6$, $Ca_2MgSi_2O_7$, $CaAl_2Si_2O_8$), respectively. Phase type corresponds to phases in the thermodynamic calculation results.

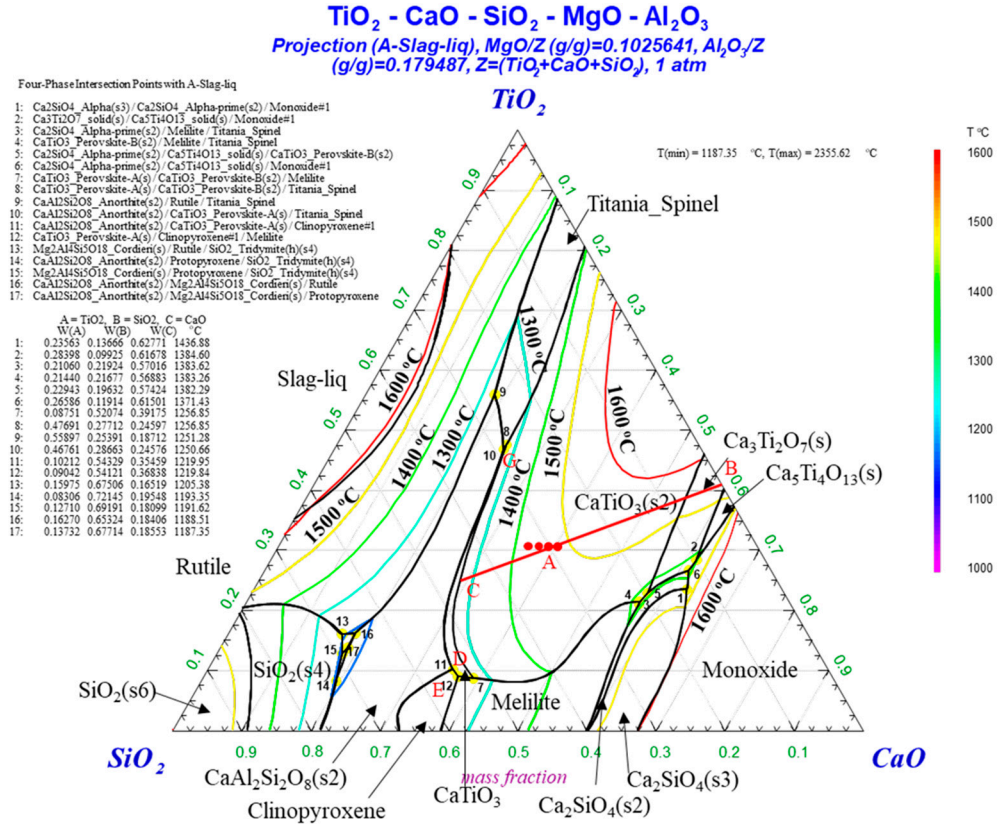

Figure 2. Pseudo ternary phase diagram of the TiO_2-CaO-SiO_2-Al_2O_3-MgO system. The red dots from left to right represent the samples with basicity of 1.1 to 1.4.

Table 3. EDS composition distribution corresponding to Figure 4a (a–d points) and Figure 4j (e point) (atom.%).

Point	Ti	Ca	O	Mg	Al	Si
a	18.70	18.93	62.38	0	0	0
b	18.09	18.39	63.52	0	0	0
c	2.45	9.73	56.45	7.09	8.93	15.35
d	0.43	0	55.84	15.05	28.68	0
e	18.53	18.79	62.68	0	0	0

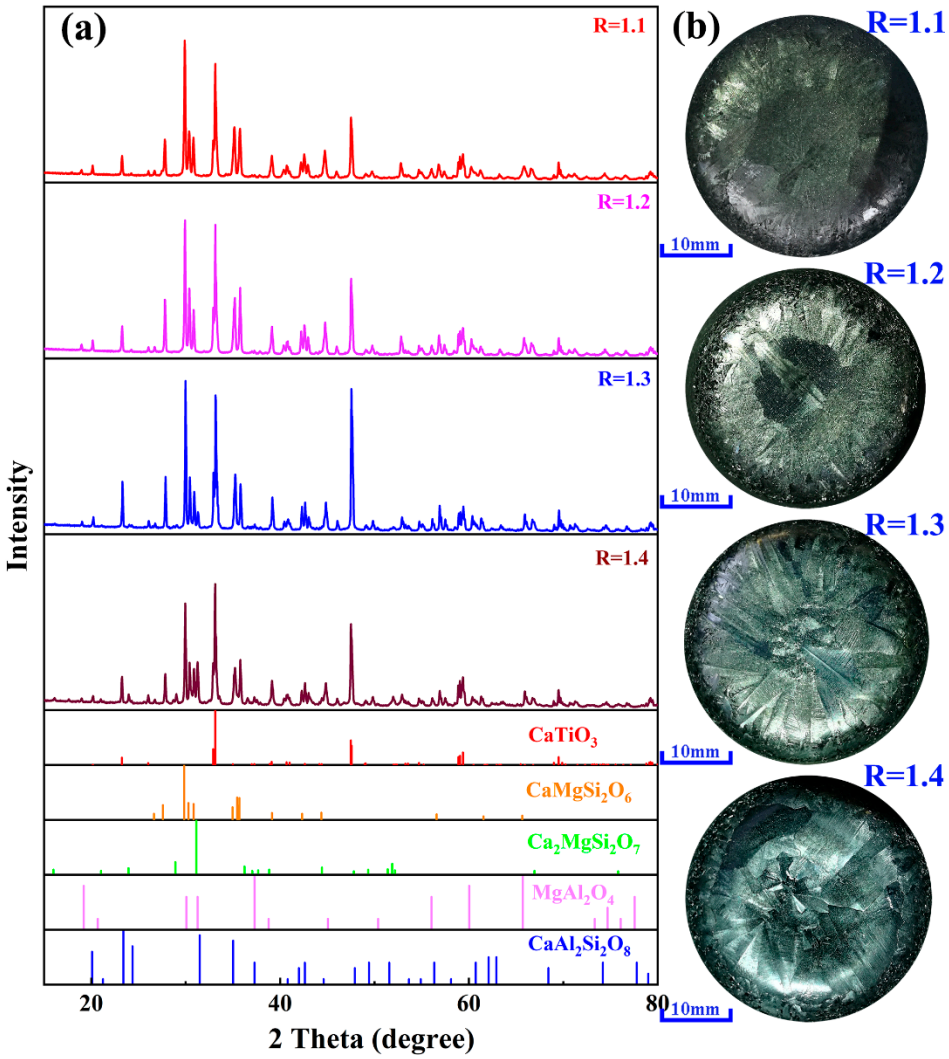

Figure 3. (**a**) X-ray Diffraction (XRD) patterns, and (**b**) the surface morphologies of the samples after cooling.

The three-dimensional morphology characteristics of the crystal were observed as shown in Figure 4g–j. Figure 4g displays that the sample is composed of numerous dendritic crystals stacking together. Figure 4h,i show that the main stem presents a spine-like appearance and the edge is blade-like. Combining BSE (Backscattered electron image) and EDS analyses (Figure 4a and Table 3), it can be obtained that the inner part of the crystal is perovskite phase and the outer part is $CaMgSi_2O_6$ phase or spinel, in Figure 4j. The reason for this is that in the crystallization process, perovskite precipitates at first, and then, $CaMgSi_2O_6$ phase and spinel start to precipitate, covering the surface of perovskite phase and filling the interdendritic space.

Finally, the electron microscope photos were preprocessed to remove the outside and record the gray level of the white perovskite area. Then, the Python OpenCV module was used to carry out image processing, gray level recognition, and contour calculation. The comparison of images before and after processing is shown in Figure 5a,b and it suggests that 200× is the most ideal magnification. Under different basicity, more than 10 photos of magnified 200× were taken to study the relationship between the amount of perovskite crystallization and basicity. The change of perovskite area as a function of basicity is shown in Figure 5c, which indicates that with the basicity increasing, the volume ratio of perovskite crystallization to the total crystallization increases. The experimental results show that perovskite is the main titania phase, and only a small amount of titania is distributed in the other phases. With the increase of basicity, the amount of perovskite precipitation increases,

which is not verified the thermodynamic calculation. The main reason for the difference between the experiment and thermodynamics is that as the basicity becomes higher, and although the concentration of TiO_2 in the slag is fixed, the amount of CaO is increased, which makes it conducive to the precipitation of perovskite kinetically. In detail, the change of perovskite content with basicity is not obvious in theoretical calculation, which is the result of equilibrium condition. Because CaO is excessive, all TiO_2 and CaO combine to form $CaTiO_3$. However, in the actual cooling process, perovskite is the first crystalline phase. According to the crystallization kinetic conditions, the higher the concentration of CaO in the liquid phase, the more conducive to the formation of $CaTiO_3$, so a higher basicity caused more perovskite formed in the experiment.

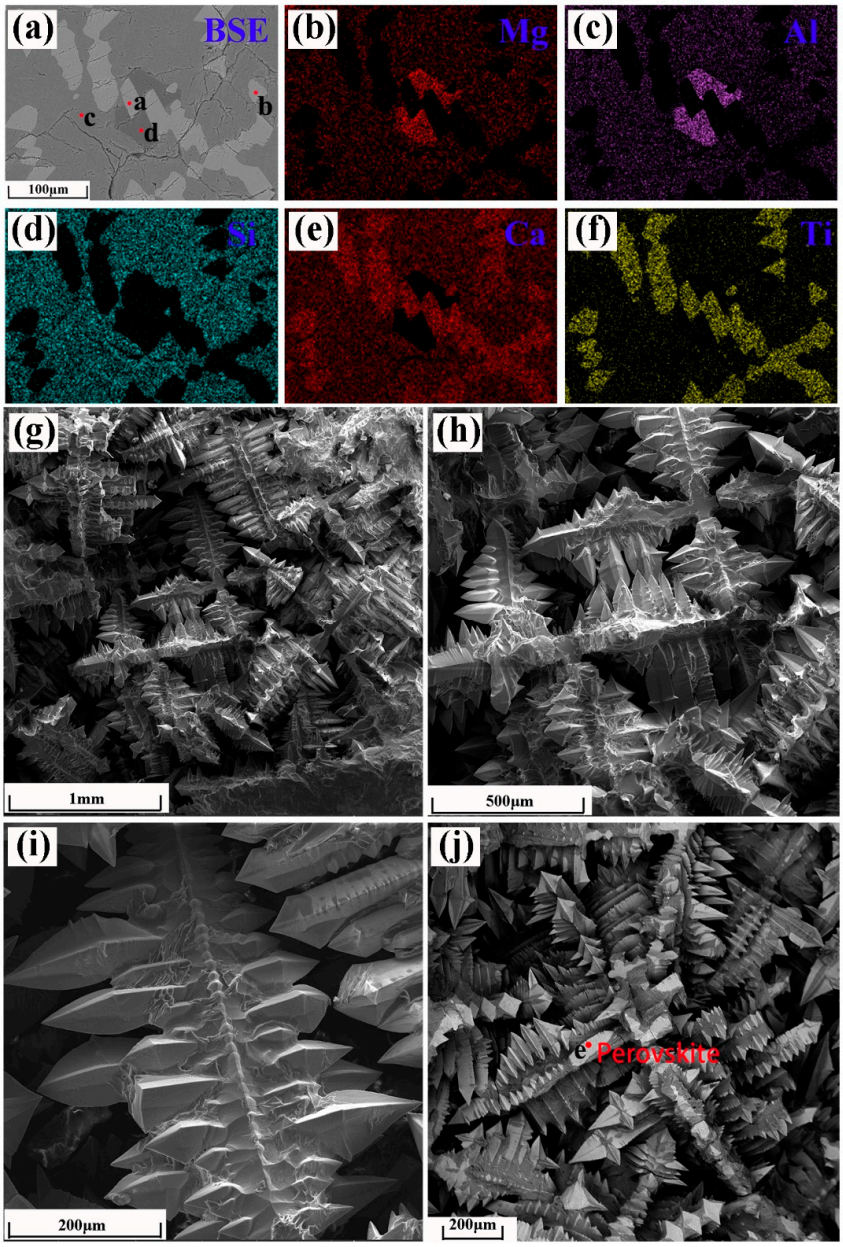

Figure 4. (**a**) Backscattered electron image (BSE) image, and (**b**–**f**) mapping of the elements corresponding to (**a**); (**g**–**j**): 3D morphologies of cooled slag with basicity of 1.3.

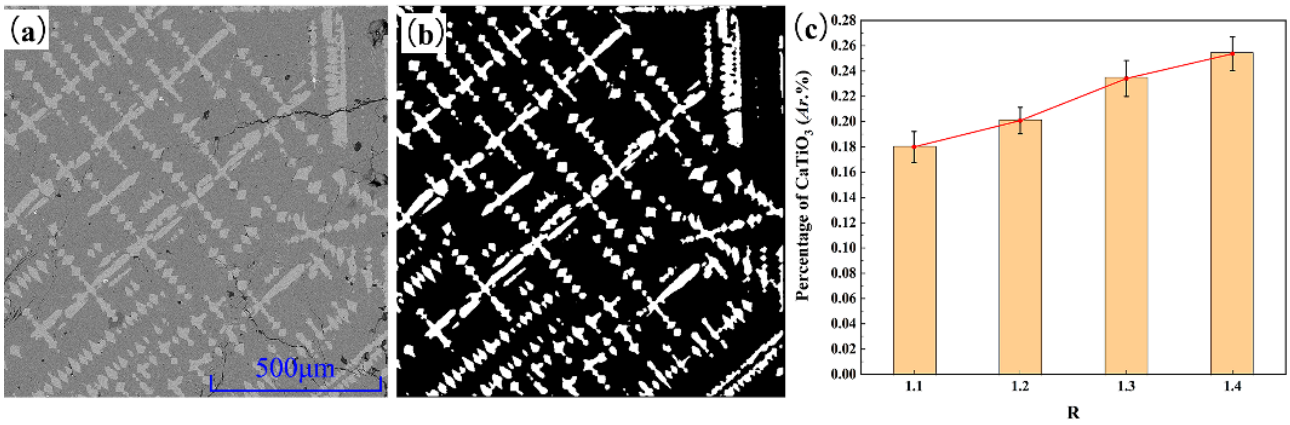

Figure 5. (**a**) The optical micrographs of cross sections of the samples with basicity of 1.1; (**b**) the recognition of $CaTiO_3$ corresponding to (**a**); (**c**) the function of $CaTiO_3$ area percentage with basicity.

3.3. The Crystallization Mechanism

The degree of supercooling affects the crystallization during the slag cooling process. Figure 6a–c show the crystal morphology of three stages: at the beginning of crystallization (around 1698 K), in the process of crystallization (around 1573 K), and completed crystallization (below 1473 K). At the beginning of crystallization, because the crucible wall has strong thermal conductivity and heat dissipation, it can be used as nucleation substrate, resulting in a large number of heterogeneous nuclei (perovskite) formed on it as shown in Figure 6a. During the crystallization process, the crystals grow continuously as the temperature decreases. The crystal morphology changes from crystal nucleus to dendrite. When the liquid phase is cooled to the precipitation temperature of the spinel phase. It begins to precipitate on the dendrite, as shown in light gray in Figure 6b. Then the liquid phase continues to change into solid phases, which accumulates on the surface of the perovskite. When the temperature drops near the liquidus temperature, the fluidity of liquid phase decreases and the intercrystalline void cannot be filled completely, and the decrease in temperature leads to the shrinkage of crystal volume and further produces holes. After the crystallization is completed, as shown in Figure 6c, the crystal morphology presents dendritic and snowflake shape.

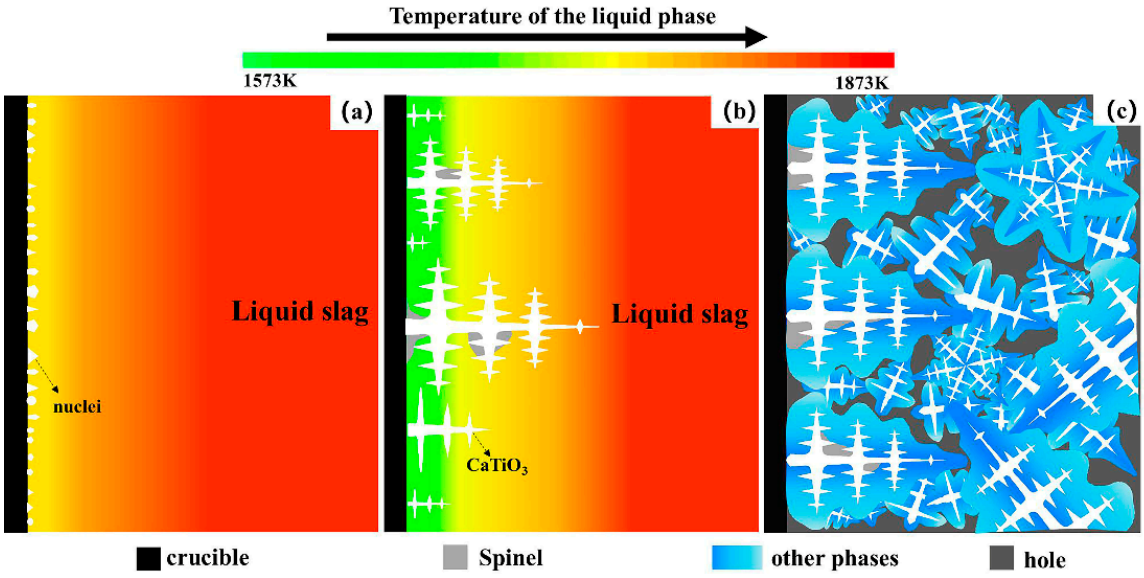

Figure 6. Schematic diagram of the (**a**) beginning of crystallization, (**b**) crystallization process, and (**c**) completion of crystallization (the change of blue depth indicates the change of titanium concentration in the phase).

4. Conclusions

In this study, the effect of basicity on the crystallization behavior of pentabasic slag was investigated thermodynamically and experimentally. Thermodynamic calculation shows that perovskite precipitates firstly from the liquid phase during the cooling process. The precipitation temperature of perovskite increases with basicity increasing, and the content of perovskite almost does not change. When the temperature drops to 1492 K, the liquid phase disappears completely and is transformed into perovskite, spinel, melilite (olivine), clinopyroxene and anorthite. The experiment shows similar results except for the amount of perovskite, which is mainly caused by kinetic conditions. The morphology of the slag at different scales was observed as well. The surface of the cooled slag is granular, vein-like, and irregular, multilaterally shaped from outside to inside. The crystal is dendritic with a spine-like trunk, and the edge is blade-like. In terms of the structure of the crystal, the inner part of it is perovskite, and the outer part is covered with a layer of other phases with spinel inlaying it. Finally, the precipitated mechanism is proposed as well. It is suggested that the basicity of slag should be properly increased to enrich titanium in $CaTiO_3$ during the processing of titanium-containing blast furnace slag.

Author Contributions: G.F. gave the early guidance. H.L., C.T., G.F. and D.H. carried out the experimental operation, XRD test, and took electron microscope photos. J.D., G.F., H.L. and X.D. analyzed the experimental and theoretical results. H.L. wrote the manuscript with help from all the coauthors. The project was initiated and conceptualized by J.D. All authors have read and agreed to the published version of the manuscript.

Funding: This research was funded by the National Natural Science Foundation of China (52074057, U1902217), the Fundamental Research Fund for the Central Universities (2020CDJGFCL004), Graduate Scientific Research and Innovation Foundation of Chongqing (CYB19003), Fok Ying Tung Education Foundation (171111), the Venture and Innovation Support Program for Chongqing Overseas Returnees (cx2019041), Joint Fund between Shenyang National Laboratory for Materials Science and State Key Laboratory of Advanced Processing and Recycling of Nonferrous Metals (18LHPY015), and Chongqing Science Fund for Distinguished Young Scholars (cstc2019jcyjjqX0024).

Data Availability Statement: Data presented in this study are available on request from the corresponding author.

Conflicts of Interest: Authors declare no conflict of interest.

References

1. Ball, C.J.; Begg, B.D.; Cookson, D.J.; Thorogood, G.J.; Vance, E.R. Structures in the system $CaTiO_3/SrTiO_3$. *J. Solid State Chem.* **1998**, *139*, 238–247. [CrossRef]
2. Liao, J.L.; Li, J.; Wang, X.D.; Zhang, Z.T. Influence of TiO_2 and basicity on viscosity of Ti bearing slag. *Ironmak. Steelmak.* **2012**, *39*, 133–139. [CrossRef]
3. Hu, M.L.; Wei, R.R.; Gao, L.Z.; Liu, L.; Bai, C.G. Effect of the Basicity on the Crystallization Behavior of Titanium Bearing Blast Furnace Slag. *High Temp. Mater. Processes.* **2018**, *37*, 193–200.
4. Liu, Y.; Zhang, Z.; Hou, G.; Yan, P. Preparation of sustainable and green cement -based composite binders with high -volume steel slag powder and ultra fine blast furnace slag powder. *J. Clean. Prod.* **2021**, *289*, 125133. [CrossRef]
5. Yang, H.; Ma, M.L.; Gao, M.L.; Xue, X.X.; Tang, Y.Q. Research on Heat Treatment Process of Foam Glass Prepared by Titania-Bearing Blast Furnace Slag. *Adv Mat Res.* **2009**, 1587–1590. [CrossRef]
6. Xiong, Y.; Aldahri, T.; Liu, W.; Chu, G.; Zhang, G.; Luo, D.; Yue, H.; Liang, B.; Li, C. Simultaneous preparation of TiO_2 and ammonium alum, and microporous SiO_2 during the mineral carbonation of titanium-bearing blast furnace slag. *Chin. J. Chem. Eng.* **2020**, *28*, 2256–2266. [CrossRef]
7. Liu, S.S.; Guo, Y.F.; Qiu, G.Z.; Jiang, T.; Chen, F. Preparation of Ti-rich material from titanium slag by activation roasting followed by acid leaching. *Trans. Nonferrous Met. Soc. China* **2013**, *23*, 1174–1178. [CrossRef]
8. Peng, B.; Wu, L.; Zhu, J.H.; Hou, Y.; Zhang, G.H. A novel method for preparing Ti_5Si_3 from Ti-bearing blast furnace slag. *Metall. Res. Technol.* **2020**, *117*, 614. [CrossRef]
9. Chen, K.Y.; Li, Y.; Meng, X.Y.; Meng, L.; Guo, Z.C. New integrated method to recover the TiO_2 component and prepare glass-ceramics from molten titanium-bearing blast furnace slag. *Ceram. Int.* **2009**, *45*, 24236–24243. [CrossRef]
10. Lai, F.F.; Leng, M.; Li, J.L.; Liu, Q.C. The Crystallization Behaviors of SiO_2-Al_2O_3-CaO-MgO-TiO_2 Glass-Ceramic Systems. *Crystals* **2020**, *10*, 794. [CrossRef]

11. Alencar, M.V.S.; Bezerra, G.V.P.; Silva, L.D.; Schneider, J.F.; Jesus Pascual, M.; Cabral, A.A. Structure, Glass Stability and Crystallization Activation Energy of SrO-CaO-B_2O_3-SiO_2 glasses doped with TiO_2. *J. Non-Cryst. Solids* **2021**, *554*, 120605. [CrossRef]
12. Kavitha, S.; Jayamani, N.; Barathi, D. Investigation on SnO_2/TiO_2 nanocomposites and their enhanced photocatalytic properties for the degradation of methylene blue under solar light irradiation. *Bull. Mater. Sci.* **2021**, *44*. [CrossRef]
13. Lei, X.F.; Xue, X.X. Preparation and characterization of perovskite-type Titania-bearing blast furnace slag photocatalyst. *Mater. Sci. Semicond. Process.* **2008**, *11*, 117–121. [CrossRef]
14. Lei, X.F.; Xue, X.X. Preparation, characterization and photocatalytic activity of sulfuric acid-modified titanium-bearing blast furnace slag. *Trans. Nonferrous Met. Soc. China* **2010**, *20*, 2294–2298. [CrossRef]
15. Jiao, H.D.; Tian, D.H.; Wang, S.; Zhu, J.; Jiao, S.Q. Direct Preparation of Titanium Alloys from Ti-Bearing Blast Furnace Slag. *J. Electrochem. Soc.* **2017**, *164*, D511–D516. [CrossRef]
16. Fan, G.Q.; Dang, J.; Lv, X.W.; Hu, M.L. Effect of basicity on the crystallization behavior of TiO_2-CaO-SiO_2 ternary system slag. *CrystEngComm* **2018**, *20*, 5422–5431. [CrossRef]
17. Zhang, R.; Dang, J.; Liu, D.; Lv, Z.P.; Fan, G.Q.; Hu, L.W. Reduction of perovskite-geikielite by methane-hydrogen gas mixture: Thermodynamic analysis and experimental results. *Sci. Total Environ.* **2020**, *699*, 13. [CrossRef] [PubMed]
18. Fan, G.Q.; Wang, M.; Dang, J.; Zhang, R.; Lv, Z.P.; He, W.C.; Lv, X.W. A novel recycling approach for efficient extraction of titanium from high-titanium-bearing blast furnace slag. *Waste Manag.* **2020**, *120*, 626–634. [CrossRef] [PubMed]
19. Li, J.; Zhang, Z.T.; Liu, L.L.; Wang, W.L.; Wang, X.D. Influence of Basicity and TiO_2 Content on the Precipitation Behavior of the Ti-bearing Blast Furnace Slags. *ISIJ Int.* **2013**, *53*, 1696–1703. [CrossRef]
20. Liu, L.; Hu, M.L.; Bai, C.G.; Lu, X.W.; Xu, Y.Z.; Deng, Q.Y. Effect of cooling rate on the crystallization behavior of perovskite in high titanium-bearing blast furnace slag. *Int. J. Miner. Metall. Mater.* **2014**, *21*, 1052–1061. [CrossRef]